Optically Pumped Frequency Reconfigurable Antenna Design

Y. Tawk, Alex R. Albrecht, S. Hemmady, Gunny Balakrishnan, and Christos G. Christodoulou

***Abstract*—This letter presents a novel frequency reconfigurable antenna design using photoconductive silicon elements as optical switches. By illuminating these silicon elements with light of suitable wavelength, their physical properties can be altered from that of a semiconductor to almost metal-like, which in turn alters the radiation properties of the antenna structure. Our work builds on similar work conducted in the past, but goes further by demonstrating a new geometry for coupling the light energy onto the silicon switches, thereby facilitating conformal integration of such reconfigurable antennas into next-generation wireless devices. In this letter, we first present a theoretical model characterizing the behavior of silicon substrate under light illumination. We then present experimental results on a stripline circuit employing a single silicon switch under light illumination and compare the theoretical model to experimental measurements. Finally, a novel frequency reconfigurable antenna design utilizing our new coupling geometry is designed, and its experimentally measured RF performance is compared to numerical simulations.**

***Index Terms*—Frequency reconfigurable antennas, optical switching, silicon processing.**

I. Introduction

THE design of reconfigurable antennas has received a lot of attention in recent years. With the increasing need for antenna bandwidth, a considerable amount of effort is given to the development of multiband antennas. Reconfigurable multiband antennas are attractive for many applications where it is desirable to have a single antenna that occupies the same real estate, but can dynamically alter its transmit and/or receive characteristics to serve multiple frequency bands. The challenge lies in the methodology adopted to connect the radiating elements together such that the resulting structure will yield the desired RF response over the frequency bands of interest [1].

The most common methodology adopted for reconfigurable antenna design is the inclusion of some form of switching circuitry. In the past, switches have been implemented using RF-MEMS [2], p-i-n diodes [3], or lumped elements [4]. Microelectromechanical systems (MEMS) switches possess good RF characteristics and can be used for low- and high-frequency applications [2]. A p-i-n diode is a versatile device and can be biased to behave like an open circuit, a short circuit, or exhibit any desired reflection coefficient in between [5]. Despite all their advantages, the use of these switching elements requires the design of an appropriate biasing network for the activation/deactivation of the switch, which can affect the antenna performance and add further complexity to the antenna structure.

In this work, photoconductive switches are used because of their superior performance as compared to MEMS, p-i-n diodes, and lumped elements. The photoconductive approach does not require the use of bias lines, which typically lie in the plane of the antenna and can interfere with the electromagnetic performance of the antenna. Also, photoconductive switches exhibit extremely fast switching speeds on the order of nanoseconds.

Some research has been done on the design of optically reconfigurable antennas. In [6], the authors used an n-type silicon switch doped with phosphorus to increase its conductivity. The authors implemented the photoconductive switch on a printed dipole antenna in order to create reconfigurability in terms of the operating frequency and radiation pattern by effectively changing the dipole arm length. In [7], planar arrays of electrically small metallic patches are connected by switches. Field-effect transistor-based electronic switches are used with optical control. The drawback in this design is that the energy lost in the switches reduces the radiating efficiency of the antenna to a point where it might prove unbeneficial for some applications. The authors of [8] introduced the concept of a photoconducting layer, behind which is placed a pixilated light source. They concluded that the realization of a metamorphic antenna using a low-cost photoconductive layer under realistic levels of illumination is extremely difficult to achieve. In [9], photoconductive switches have been used to model a fragmented bowtie antenna. The illumination of a small section of a variable conducting material using a LED was discussed in [10]. An optically controlled frequency reconfigurable microstrip antenna was implemented in [11]. The authors used the idea of shortening the slot inside the antenna patch in order to make the antenna change its electrical length. This has the effect of producing a different resonant frequency.

In this letter, a different design of an optically controlled frequency reconfigurable antenna is presented. Here, the photoconductive switches are activated by laser light (of suitable wavelength) that is coupled through an optical fiber and extends from the ground plane to just underneath the photoconducting element placed on the radiating face of the antenna structure. Such a construction allows for easy integration of such antenna designs into conformal packaging for wireless devices. Our letter is organized in the following manner. In Section II, we present

Manuscript received January 31, 2010; revised March 22, 2010; accepted March 25, 2010. Date of publication April 05, 2010; date of current version April 19, 2010.

Y. Tawk, S. Hemmady, and C. G. Christodoulou are with the Electrical and Computer Engineering Department, University of New Mexico, Albuquerque, NM 87131-0001 USA (e-mail: yatawk@ece.unm.edu; shemmady@unm.edu; christos@ece.unm.edu).

A. R. Albrecht and G. Balakrishnan are with the Center for High Technology Materials, University of New Mexico, , Albuquerque, NM 87106 USA (e-mail: alex2@unm.edu; gunny@unm.edu)

Color versions of one or more of the figures in this letter are available online at http://ieeexplore.ieee.org.

Digital Object Identifier 10.1109/LAWP.2010.2047373

TABLE I
MOBILITY PARAMETERS FOR SILICON

Parameter	Electrons	Holes
μ_{min}	52.2	44.9
μ_{max}	1417	471
N_{ref}	$9.68*10^{16}$	$2.23*10^{17}$
α	0.68	0.719

TABLE II
RELATION BETWEEN POWER LEVELS AND CARRIER CONCENTRATION

Power Level (mW)	Total Electrons Concentration (cm^{-3})
0	$1*10^{15}$
50	$6.8*10^{15}$
120	$1.5*10^{16}$
212	$2.6*10^{16}$

a theoretical model for the change in the electromagnetic properties of silicon material as a function of the incident laser light power. Section III then discusses an experiment used to validate this theoretical model. Having validated the theoretical model, in Section IV, we then show an example of a dual-band frequency reconfigurable antenna using photoconductive silicon switches. Section V concludes the letter with a discussion on the applicability of this work and possible future trends.

II. MODELING THE RF PROPERTIES OF THE SILICON UNDER LIGHT ILLUMINATION

Under illumination by light of suitable wavelength, the mobility of charge in a semiconducting material decreases, but its density increases. This increase in the charge carrier density results in a general increase in the conductivity of a semiconducting material [12]. In general, the dependence of the mobility of electrons and holes in silicon can be described by the following equation [13]:

$$\mu = \mu_{\min} + \frac{\mu_{\max} - \mu_{\min}}{1 + \left(\frac{N}{N_{\text{ref}}}\right)^{\alpha}} \tag{1}$$

where μ is the electrons or holes mobility ($\text{cm}^2/\text{V}\cdot\text{s}$), and $\mu_{\min}$, $\mu_{\max}$, N_{ref} (cm^{-3}), and α are the fitted coefficients given in Table I.

The first step is to derive the total carrier concentration that is a function of the incident laser power level. The silicon piece under investigation in this work is a doped n-type material with an initial concentration of 10^{15} cm^{-3} and has the dimension of 1×1 mm^2 and a thickness of 0.28 mm. The results for the charge carrier concentration as a function of incident power level are summarized in Table II.

The change in the dielectric constant of the silicon piece due to the increase in the total carrier concentration is given by [14]

$$\varepsilon_r = \varepsilon_{\text{L}} + \frac{ne^2}{m^* \varepsilon_o \left(-w^2 + j\frac{w}{\tau}\right)} \tag{2}$$

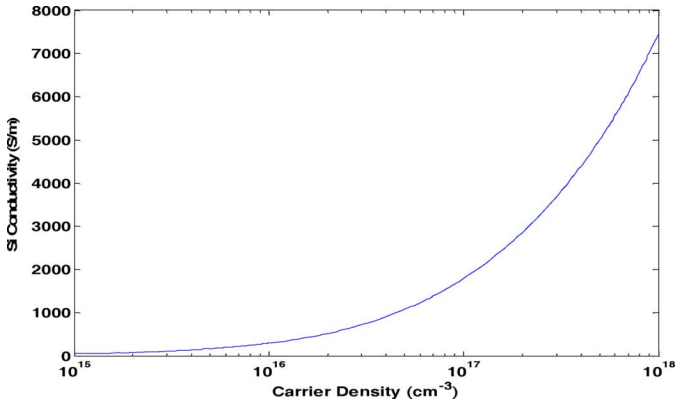

Fig. 1. Change in the silicon conductivity.

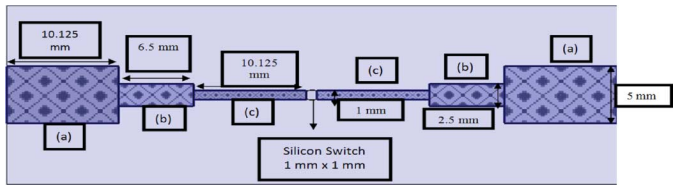

Fig. 2. The transmission line structure to test the theoretical model in Section II.

TABLE III
PHYSICAL PROPERTIES OF SILICON AT 12 GHZ

Power Level (mW)	Conductivity	Loss Tangent	Dielectric Constant
0	52	0.58	11.85
50	211	2.56	10.94
120	409	5.5	9.87
212	622	9.29	8.88

where:

- n is the electrons or holes concentration (cm^{-3});
- q is the electron charge ($\approx 1.602 * 10^{-19}$ C);
- m^* is the charge effective mass (kg);
- w is the operating frequency (Hz);
- τ is the collision time ($\approx 10^{-3}$ s);
- ε_{L} is the dielectric constant of the silicon (≈ 11.9).

From (2), the physical properties such as the conductivity (σ), the loss tangent ($\tan\ \delta$), and the dielectric constant (ε) of the silicon under different power levels can be derived [12]. This is summarized in Table III. It can be seen that as the carrier concentration increases, the conductivity of the silicon also increases, and its dielectric constant decreases. However, the silicon becomes lossier due to the increase in its dielectric loss tangent. The trend of variation of the silicon RF+DC conductivity is shown in Fig. 1.

III. OPTICALLY SWITCHED TRANSMISSION LINE

In Section II, we described a model for n-type silicon under different illumination. To test this model, we designed a transmission line shown in Fig. 2. A silicon switch is placed in the

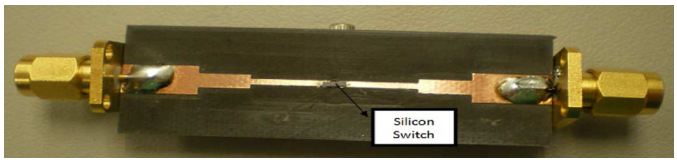

Fig. 3. The fabricated prototype.

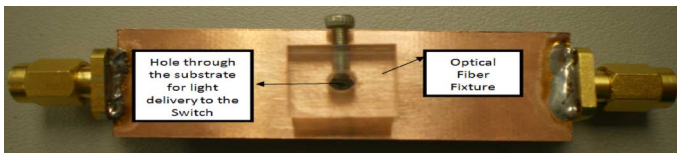

Fig. 4. The backside view of the fabricated prototype.

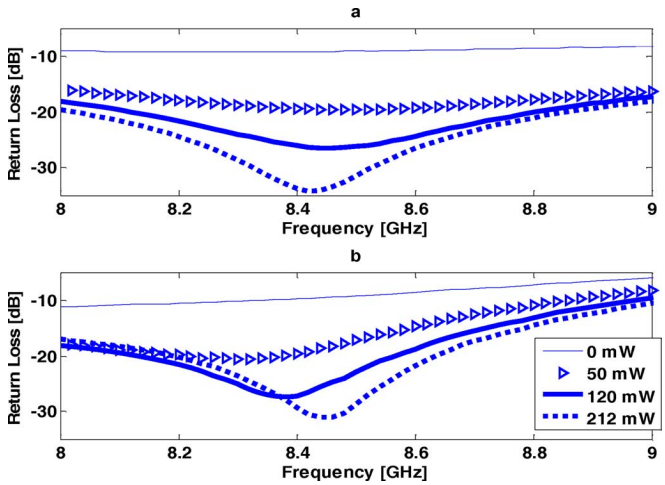

Fig. 5. (a) The simulated and (b) the measured return loss.

middle of the structure. The chosen substrate is Rogers Duroid with a dielectric constant of 2.2 and a height of 1.6 mm.

The stripline structures on either side of the silicon switch are identical. The sections labeled (a) in Fig. 2 have a characteristic impedance of 50 Ω. The silicon switch used has a width of 1 mm. Assuming the silicon switch was a perfect metal, the 1-mm width would correspond to an impedance of 118 Ω. Therefore, the transmission line [parts (c)] has an impedance of 118 Ω. A quarter-wavelength transformer [parts (b)] is used to match the two transmission lines sections [parts (a) and (c)]. It has a length of 6.5 mm, which translates to a resonant frequency of 8.4 GHz. The fabricated prototype is shown in Fig. 3. The light (from an 808-nm laser diode) is delivered to the silicon switch via an optical fiber cable. It is placed underneath the substrate and held via a plastic fixture as shown in Fig. 4.

The return loss for this transmission line structure for different power levels shows that the silicon acts as a switch. As the power level increases, the conductivity of the silicon piece increases, thereby reducing the reflection loss. At 212 mW, a minimal reflection is observed. The simulated and the measured transmission line return loss is shown in Fig. 5. By comparing both plots, one can notice that a good agreement is found between both data. In such structure, it is instructive to also look at the transmission between ports 1 and 2. The measured transmission is shown in Fig. 6. As expected, the higher the power level, the more RF signal is being delivered to the load. In this experiment, we assume that the losses in the fiber are negligible and that all the laser energy is coupled to the silicon switch. This

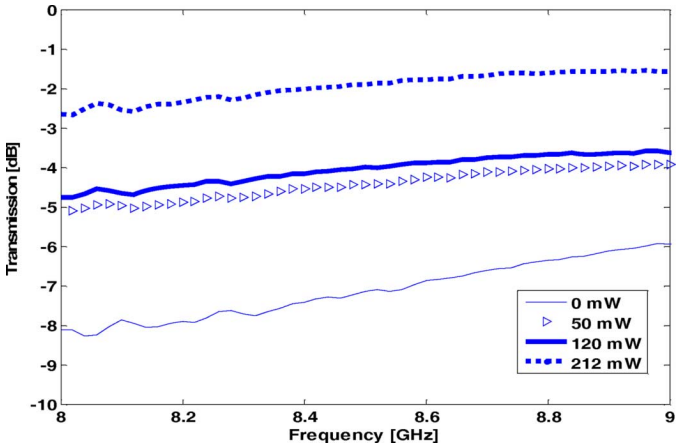

Fig. 6. The measured transmission between port 1 and port 2.

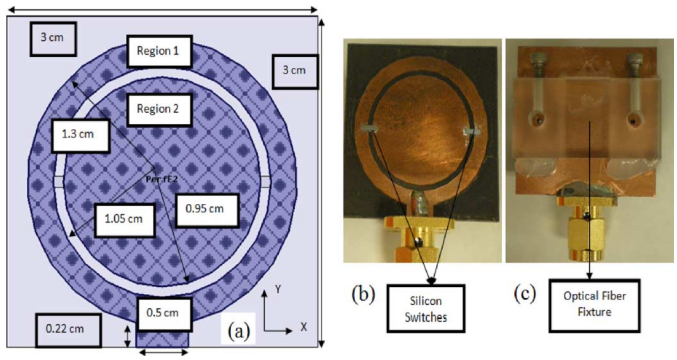

Fig. 7. (a) The antenna dimensions. (b) The antenna top layer. (c) The antenna bottom part.

experiment enables us to conclude that the silicon piece can act as a RF switch and can be used in the design of reconfigurable antennas.

IV. Frequency Reconfigurable Antenna Design

Following the experiment in Section II, an optically reconfigurable antenna was designed and tested using the same silicon switch. The antenna structure consists of an outer circular annular ring (Region 1) and an inner circular patch (Region 2). Both structures are separated via a 1-mm gap and connected together via two silicon pieces that act as the RF switches. The dimensions of the different parts of the antenna structure are shown in Fig. 7(a). The top view of the fabricated antenna topology is shown in Fig. 7(b). The bottom view of the antenna structure is shown in Fig. 7(c). The chosen substrate is Rogers Duroid with a dielectric constant of 2.2 and a height of 1.6 mm. The light (from an 808-nm laser diode) is delivered to the silicon switch via an optical fiber cable. It is placed underneath the substrate and held via a plastic fixture. To couple light into the silicon switch, two holes of radius 1 mm each are drilled into the substrate, as shown in Fig. 7(c). We again make the same assumption that the losses in the fiber are negligible and that all the laser energy is coupled to the silicon switch.

When the two silicon switches are not illuminated by a laser light (OFF state), only the circular ring (Region 1) is fed. This results in an antenna resonance between 18 and 19 GHz. Upon activation of the silicon switches, a new resonance begins to appear at 12 GHz. This is due to the mutual coupling between regions 1 and 2. Since the combined regions now represent

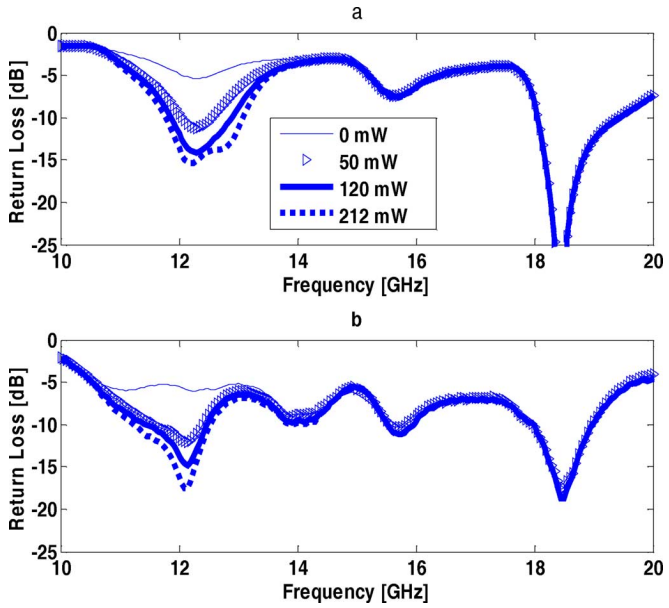

Fig. 8. (a) The simulated and (b) the measured return loss.

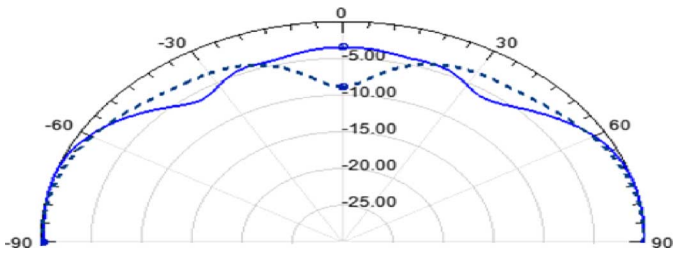

Fig. 9. The computed radiation pattern at 18.4 GHz (solid line) and 12.2 GHz (dotted line) in the xz plane for the antenna structure in Fig. 7.

an antenna with larger metallized surface area, the resonant frequency shifts lower. The simulated and the measured antenna return losses for the different power levels are shown in Fig. 8(a) and (b). As the pumped power increases, the RF conductivity of the silicon switch increases, thereby reducing the impedance mismatch between regions 1 and 2, and subsequently yields deeper resonances. By comparing both plots, one can observe a good qualitative agreement between the simulated and the measured data in terms of the frequency dependence of the observed resonances.

The simulated antenna radiation patterns at $\Phi = 0^\circ$ (xz plane) when both switches are OFF ($\mathrm{f} = 18.4$ GHz, solid line) and when both switches are ON ($\mathrm{f} = 12.2$ GHz, dotted line) for a 212-mW incident laser power are shown in Fig. 9. For both cases, the antenna preserves its omnidirectional property. The boresight directivity gain of the antenna was then determined using the reflection measurement technique in [15]. By placing a ground plane of dimensions 25×25 cm^2 10 cm in front of the antenna, a VSWR value of 1.149 at 18.3 GHz was obtained in the case where both switches were OFF, and $\mathrm{VSWR} = 1.106$ at 11.8 GHz with both switches ON. This translates to a measured boresight gain of 10.26 (10.87 dB simulated) and 5.42 dB (5.75 dB simulated). The increase in the material losses introduced by the silicon switches for increasing pumped laser power levels results in reduced radiation efficiency of the antenna structure and correspondingly reduces the boresight gain values.

V. Conclusion

This letter presents a new reconfigurable antenna design based on optical switching. The electromagnetic behavior of the silicon switch under illumination by light of suitable wavelength was modeled, and a switched transmission line was investigated. Next, a dual-band antenna was designed and tested. In this letter, the choice of the frequency range for the antenna is arbitrary and serves to only validate the proof of concept for our approach. The physical geometry for the coupling of light energy onto the silicon switch adopted here allows for such antenna designs to be easily integrated into compact packages that can be included in next-generation wireless devices. Furthermore, our antenna designs can be easily tweaked to include frequency bands corresponding to established wireless standards such as GSM, CDMA, WiMAX, etc. For future work, one can explore methods to decrease the required pumped laser power by decreasing the dimension of the silicon switches and/or investigating other materials with faster switching speeds.

References

[1] A. Patnaik, D. E. Anagnostou, C. G. Christodoulou, and J. C. Lyke, "A frequency reconfigurable antenna design using neural networks," in *Proc. IEEE Antennas Propag. Soc. Int. Symp.*, Jul. 3–8, 2005, vol. 2A, pp. 409–412.

[2] D. E. Anagnostou, G. Zheng, M. T. Chryssomallis, J. C. Lyke, G. E. Ponchak, J. Papapolymerou, and C. G. Christodoulou, "Design, fabrication, and measurement of an RFMEMS-based self-similar reconfigurable antenna," *IEEE Trans. Antennas Propag.*, vol. 54, no. 2, pp. 422–432, Feb. 2006.

[3] M. I. Lai, T. Y. Wu, J. C. Hsieh, C. H. Wang, and S. K. Jeng, "Design of reconfigurable antennas based on an L-shaped slot and PIN diodes for compact wireless devices," *IET Microw., Antennas Propag.*, vol. 3, pp. 47–54, 2009.

[4] N. Behdad and K. Sarabandi, "Dual-band reconfigurable antenna with a very wide tunability range," *IEEE Trans. Antennas Propag.*, vol. 54, no. 2, pp. 409–416, Feb. 2006.

[5] A. C. K. Mak, C. R. Rowell, R. D. Murch, and C. L. Mak, "Reconfigurable multiband antenna designs for wireless communication devices," *IEEE Trans. Antennas Propag.*, vol. 55, no. 7, pp. 1919–1928, Jul. 2007.

[6] C. J. Panagamuwa, A. Chauraya, and J. C. Vardaxoglou, "Frequency and beam reconfigurable antenna using photoconducting switches," *IEEE Trans. Antennas Propag.*, vol. 54, no. 2, pt. 1, pp. 449–454, Feb. 2006.

[7] L. N. Pringle *et al.*, "A reconfigurable aperture antenna based on switched links between electrically small metallic patches," *IEEE Trans. Antennas Propag.*, vol. 52, no. 6, pp. 1434–1445, Jun. 2004.

[8] R. P. Tuffin, I. C. Sage, B. J. Hughes, and G. J. Ball, "Electronically controlled metamorphic antenna," in *Proc. 4th EMRS DTC*, 2007, p. A9.

[9] B. J. Hughes, I. C. Sage, and G. J. Ball, "Optically controlled metamorphic antenna," in *Proc. 5th EMRS DTC*, 2008, p. B24.

[10] R. L. Haupt and J. R. Flemish, "Reconfigurable and adaptive antennas using materials with variable conductivity," in *Proc. 2nd NASA Conf. Adaptive Hardware Syst.*, 2007, pp. 20–26.

[11] R. N. Lavalle and B. A. Lail, "Optically-controlled reconfigurable microstrip patch antenna," in *Proc. IEEE Antennas Propag. Soc. Symp.*, Jul. 5–11, 2008, pp. 1–4.

[12] C. A. Balanis, *Advanced Engineering Electromagnetic*. New York: Wiley, 1989.

[13] R. S. Muller, T. I. Kamins, and M. Chan, *Device Electronics for Integrated Circuits*, 3rd ed. Hoboken, NJ: Wiley, 2003.

[14] C. H. Lee, P. S. Mak, and A. P. DeFonzo, "Optical control of millimeter-wave propagation in dielectric waveguides," *IEEE J. Quantum Electron.*, vol. QE-16, no. 3, pp. 277–288, Mar. 1980.

[15] S. Silver, "Microwave antenna theory and design," *IEE Electromagn. Waves Series*, pp. 585–586, 1997.